JOURNAL OF NANO- AND ELECTRONIC PHYSICS
Vol. 18 No 4, 04014(6pp) (2026)
ЖУРНАЛ НАНО- ТА ЕЛЕКТРОННОЇ ФІЗИКИ
Том 18 № 4, 04014(6cc) (2026)

OPEN ACCESS

REGULAR ARTICLE

Design of FSS-Based Gain-Enhanced Wideband Srichakra-Shaped Antenna for Point-to-Point Microwave Data Links

Ghali Srinivasa Rao[1,*], B.T.P. Madhav[1], Y. Usha Devi[1], Geetha Reddy Yenna[2], K Jyostna[3], Lokesh Raju V[4]

[1] ALRC Research Centre, Department of ECE, Koneru Lakshmaiah Education Foundation, Guntur, 522302 Andhra Pradesh, India
[2] Malla Reddy Engineering College for Women (MRECW), Hyderabad, India
[3] Department of ECE, VNR VJIET, Hyderabad, India
[4] Department of ECE, Adithya Institute of Technology and Management (AITM), Tekkali, AP, India

(Received 28 March 2026; revised manuscript received 16 August 2026; published online 21 August 2026)

A compact Srichakra-inspired planar antenna combined with a frequency-selective surface (FSS) is implemented for wideband point-to-point microwave data-link applications. The proposed antenna employs a Rogers RO4350B dielectric occupying a compact volume of 46 × 51.5 × 0.3 mm³. To enhance forward radiation, a fractal-inspired spiral resonator FSS is employed as a passive superstrate. The FSS unit cell is formed by a 12 × 12 mm² periodicity and is implemented on a 0.4 mm RO4350B substrate. A 6 × 6 FSS array is formed, resulting in an overall dimension of 78 × 78 mm². This arrangement functions as a compact broadband partially reflective surface. The FSS redirects backward radiation toward the forward half-space through constructive field interaction. As a result, a stable gain enhancement is achieved over a wide operating frequency range. The realised gain increases from 6.9 dBi without FSS to a peak value of 11.2 dBi with FSS. This corresponds to a maximum gain improvement of about 3 dB. The antenna preserves stable impedance matching & radiation behavior after FSS integration. Consistently high gain is observed across the 5-20 GHz band. The use of low-loss materials and a passive enhancement mechanism ensure high radiation efficiency. Overall, the developed antenna offers a compact, wideband, and high-gain design suitable for point-to-point microwave data-link communication systems.

Keywords: FSS (Frequency selective surface), Gain enhancement, Microwave data-link communication, Point-to-point communication, Wideband antenna.

DOI: 10.21272/jnep.18(4).04014 PACS number: 84.40.Ba

1. INTRODUCTION

A (FSS) frequency-selective surface is a periodic arrangement of conductive or dielectric elements used to control electromagnetic wave propagation. Electromagnetic waves are based on frequency and polarization, & is commonly employed as a reflector or superstrate to enhance antenna gain & front-to-back ratio. Gain enhancement strengthens the directional radiation capability of the antenna toward a desired angular region, thereby improving link margin, coverage distance, and signal reliability. Microwave point-to-point data-link systems rely on highly directional high-gain antennas for efficient transmission between a single transmitter and receiver, ensuring high data rates, low interference, and robust connectivity. Wideband antennas further support multiple services across a broad frequency spectrum while maintaining stable radiation and impedance performance.

Microstrip patch antennas are widely adopted in modern wireless systems due to their low profile, light weight, and ease of fabrication [1]. In [2], a compact flower-shaped fractal antenna on FR-4 provides six-band operation for modern wireless and satellite systems. An M-shaped conformal antenna supported by an FSS is also reported to achieve significant broadband gain improvement. In [3], the FSS delivers 22 % gain and 12 % efficiency improvement with strong simulation-measurement agreement, while a compact tri-wideband Sierpinski fractal antenna with a modified ground is also presented for wireless applications. In [4], a tri-wideband antenna covering 2.19-11.32 GHz is reported for multiple wireless bands. A compact CPW-fed circular monopole with EBG loading is also presented to boost gain and efficiency. In [5], an antenna operating over 1.5-3.6 GHz and 4.8-15 GHz is reported, supporting GPS, LTE, Bluetooth, Wi-Fi, WLAN, X-band, & satellite communication. In [6], a UWB semicircular monopole with a slotted ground and a 6 × 6 FSS reflector achieves a 4 dB average gain improvement, reaching a peak gain of 8.3 dB over the 3-11 GHz band. In [7], a systematic review highlights the effectiveness of FSS reflectors for UWB gain enhancement, improved directivity, and interference suppression, while maintaining stable – 10 dB return-loss performance. In [8], a CPW-fed UWB antenna backed by a 5 × 5 FSS (50 × 50 mm²) is presented to improve wideband gain. With a 9 mm air gap, the

* Correspondence e-mail: srinivas.bharadwaja@gmail.com

Cite this article as: G.S. Rao, et al., *J. Nano- Electron. Phys.* 18 No 4, 04014 (2026) https://doi.org/10.21272/jnep.18(4).04014

bandwidth increases to 3 to 18 GHz & the peak gain reaches 10.5 dBi. In [9], integrating a 6 × 6 FSS with a star-shaped antenna enhances C-band vehicular communication, widening the bandwidth to 3.35-8.34 GHz and raising the gain to 9.6 dB at 5.9 GHz & 10.0 dB at 7.3 GHz. In [10], a fractal-based wearable button antenna on an FR-4 substrate using a coaxially fed slotted circular patch is presented, operating over 4.1-4.64, 7.19-8.03, and 8.85-9.67 GHz. Enhanced bandwidth and gain are achieved through optimized fractal circular slot design. In [11], an X-band triangular slot antenna using a merged dual rhombic loop (MDRL) FSS is reported for enhanced boresight gain. At 8.2 GHz, it achieves a 650 MHz bandwidth and an 8.5 dB peak gain, with 4.5 dB contributed by the FSS. In [12], a 30 × 24 mm^2 Koch-curve hexagonal fractal antenna achieves six resonances (3.4-15 GHz) with a 10.42-GHz (99.43 %) bandwidth using DGS, parasitic, and EC-SRRs. In [13], a Srichakra-shaped wideband fractal antenna for S-, C-, X-, & Ku-bands achieves a peak gain of 8.66 dB with 95 % radiation efficiency on RT/duroid (RO4350B). In [14], a triband H-shaped antenna for C/X/Ku-J bands achieves 7.1 dB gain with − 16.5 dB return loss at 15 GHz, operating over 6.1-6.6, 10.9-11.1, and 13.1-16 GHz.

The proposed Srichakra-shaped wideband monopole antenna employs a fractal-inspired spiral FSS arranged in a 6 × 6 arrays beneath the radiator. Acting as a partially reflective surface, the FSS redirects backward radiation toward the forward direction through constructive interference, resulting in ~ 3 dB gain enhancement, improved directivity, and better overall link performance.

2. EVOLUTION OF THE PROPOSED ANTENNA GEOMETRY

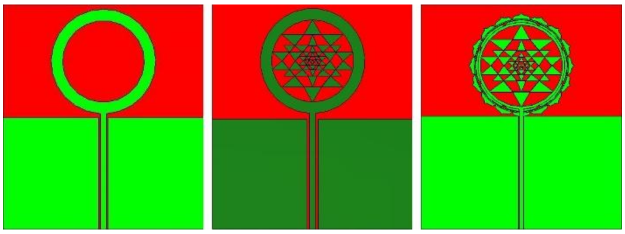

a b c

Fig. 1 – Progressive iterations of the suggested antenna geometry

Fig. 1 shows the antenna geometry that evolves over three iterations to achieve wideband operation and improved radiation performance. A circular monopole with partial ground excites the fundamental resonance, followed by a fractal radiator that introduces multiple current paths for bandwidth enhancement. In the final stage, Srichakra-inspired lotus petals are added to improve current distribution, impedance matching, and radiation efficiency. Reflection-coefficient and surface-current analyses confirm progressive improvement, and the final geometry exhibits superior wideband performance. The antenna dimensions are retained from the validated design in [13] to clearly emphasize the gain enhancement introduced by the proposed FSS.

Fig. 2(a) shows that the final antenna iteration exhibits multiple resonances at 3.2, 5.1, 7.4, 10.2, 13.8, 17.2, and 20.5 GHz, with S_{11} < – 15 dB. A continuous – 10 dB impedance bandwidth of 3-22 GHz is achieved, corresponding to an absolute bandwidth of about 19 GHz and a fractional bandwidth of ~ 190 %. Fig. 2(b) illustrates the influence of feed width variation on impedance matching. For W_f = 0.7 mm, the antenna attains the deepest return-loss minima (≈ − 30 dB) and a continuous wideband response from 3-22 GHz, whereas W_f = 0.5 mm and 0.6 mm introduce impedance mismatches with shallower nulls (≈ − 15 to – 20 dB) and minor bandwidth discontinuities. Hence, W_f = 0.7 mm is selected as the optimal feed width for superior ultra-wideband performance.

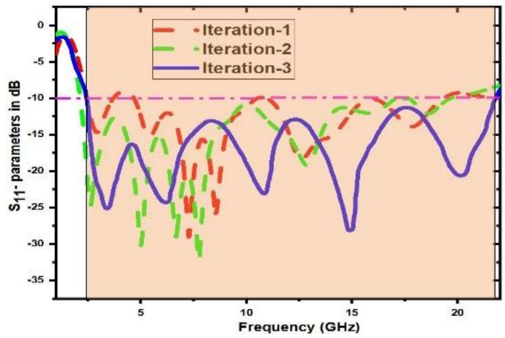

a

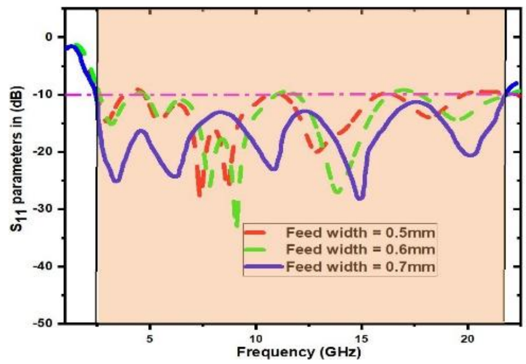

b

Fig. 2 – Parametric investigation and iterative reflection coefficient analysis of the proposed antenna. (a) Iteration-based S_{11} response, (b) Feed width study

3. DESIGN OF THE PROPOSED FRACTAL SPIRAL FSS UNIT CELL

Fig. 3(a) illustrates the suggested fractal spiral FSS unit cell, and Fig. 3(b) shows a compact dimension of 12 × 12 mm^2. The spiral metallic geometry introduces multiple current paths, enabling wideband electromagnetic resonance. This unit cell serves as the fundamental building block of the FSS array and governs its reflection characteristics, making its optimised design critical for effective antenna gain enhancement.

The proposed FSS consists of a compact fractal spiral unit cell designed to provide strong electromagnetic resonance and broadband reflective behaviour, with its geometry controlling the reflection phase and gain enhancement capability. A 6 × 6 FSS array (78 × 78 mm^2) placed beneath the antenna acts as a partially reflective surface, redirecting backward radiation toward the forward direction through constructive interference, resulting in a boresight gain enhancement of 3 dB without increasing input power.

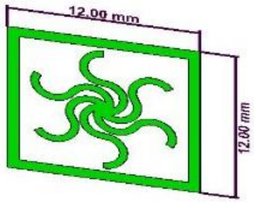

a

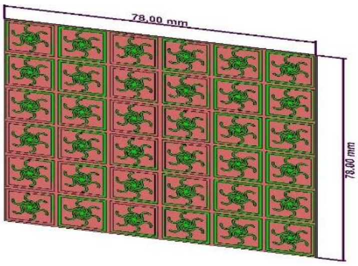

b

Fig. 3 – Geometry proposed for gain-enhancement FSS: (a) Fractal spiral single unit cell with dimensions, (b) 6 × 6 FSS configuration with overall dimensions

Consequently, the antenna exhibits improved gain, directivity, front-to-back ratio, and radiation efficiency, with efficiency increasing from 60-85 % without FSS to 70-95 % with FSS over the 2-20 GHz band, confirming the broadband effectiveness of the proposed FSS.

4. ARRANGEMENT OF THE SRICHAKRA-SHAPED ANTENNA AT THE CENTER OF THE FSS STRUCTURE

When the air gap satisfies the Fabry-Pérot resonance condition, the wave reflected from the FSS combines constructively with the directly radiated wave, thereby enhancing boresight radiation and suppressing backward radiation.

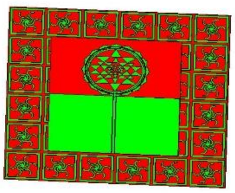

a

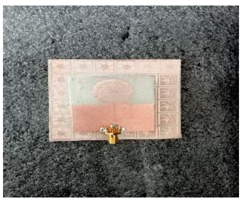

b

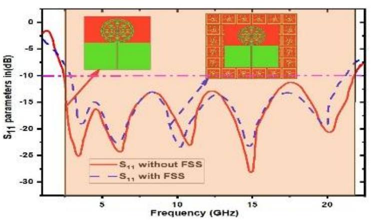

(c)

Fig. 4 – (a) arrangement of srichakra-shaped antenna at the center of the FSS structure, (b) prototype models arrangement, (c) S_{11} variations with FSS

The proposed antenna employs a superstrate-type FSS, consisting of a finite 6 × 6 fractal spiral array placed above the Srichakra-shaped monopole at an optimized air gap. The FSS acts as a partially reflective surface (PRS) with stable reflection magnitude and phase over a wide band, enabling broadband gain enhancement. Its finite aperture (78 × 78 mm^2) converts the spherical wavefront into a quasi-planar wavefront, improving gain, FBR ratio, & radiation efficiency. The antenna-FSS system forms a Fabry-Pérot cavity with an optimized air gap of $h = 20$ mm, where maximum boresight gain is achieved.

$$2\beta h + \phi_r + \phi_g = 2$$

Where $\beta = \frac{2\pi}{\lambda}$, is the free-space phase constant, ϕ_r is the FSS reflection phase, ϕ_g is the antenna ground-plane reflection phase, and mmm is the resonance mode. When this condition is satisfied, the wave reflected from the FSS returns in phase with the directly radiated wave, producing constructive interference and enhanced forward gain. Fig. 4(a)-(c) shows that without the FSS, the antenna resonates at 3.2, 5.1, 7.6, 10.2, 14.8, and 18.4 GHz with a minimum S_{11} of − 30 to −35 dB and a – 10 dB bandwidth of 2.9-20.5 GHz, confirming ultra-wideband operation. After FSS integration, the resonances slightly shift to 3.0, 4.9, 7.3, 9.8, 14.3, and 18.0 GHz, while the – 10 dB bandwidth is preserved from 3.1-20.0 GHz with S_{11} of − 20 to – 28 dB. The antenna achieves a fractional bandwidth of 150.4 % without FSS and 146.3 % with FSS, indicating only a marginal bandwidth reduction due to Fabry-Pérot loading while maintaining significant gain enhancement.

5. GAIN ENHANCEMENT PERFORMANCE WITH FSS

After integrating the FSS superstrate, the realized gain of the antenna is evaluated across the entire frequency band to quantify the enhancement. The comparative gain response clearly demonstrates improved forward radiation due to the FSS, this verifies that the antenna is well suited for wideband and high-gain applications.

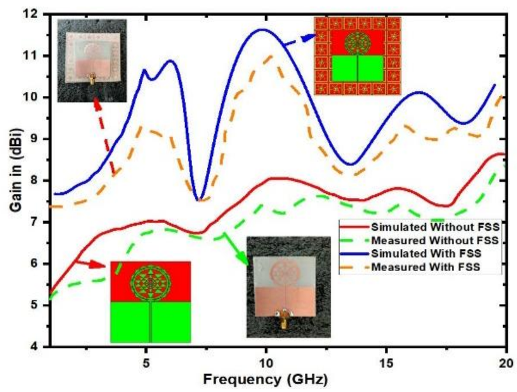

a

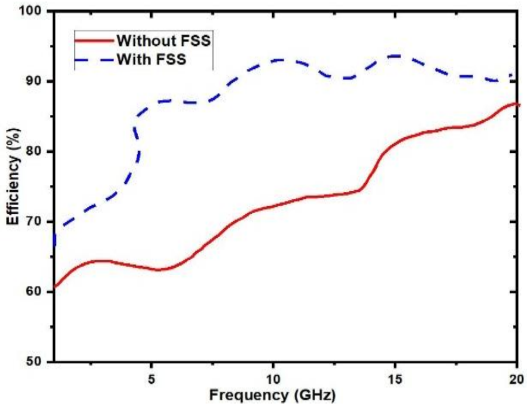

b

Fig. 5 – Comparison of the antenna's gain & efficiency with & without the integrated FSS superstrate. (a) Peak gain (b) Efficiency

Fig. 5 presents the realised gain comparison of the antenna with & without the FSS over 2-20 GHz. Without the FSS, the gain varies from 5.3 dBi at 2 GHz to 8.6 dBi at 20 GHz, averaging 7-8 dBi. With the 6 × 6 fractals spiral FSS, the gain increases from 7.6 dBi at 2 GHz to a peak of 11.6-11.7 dBi at 10-11 GHz, achieving enhancements of 3.5 dB (5 GHz), 3.6 dB (10 GHz), 2.3 dB (15 GHz), and 1.6 dB (20 GHz). The average enhancement of 2-3.5 dB across the ultra-wideband confirms the effectiveness of the FSS as a partially reflective superstrate, achieved through constructive interference that improves effective aperture and boresight directivity without increasing antenna size or input power.

6. FAR-FIELD RADIATION PATTERN RESULTS

The radiation characteristics are analyzed to evaluate the antennas in directional behavior. Normalised *E*- and *H*-plane patterns at selected resonant frequencies illustrate the beam shape and main-lobe orientation.

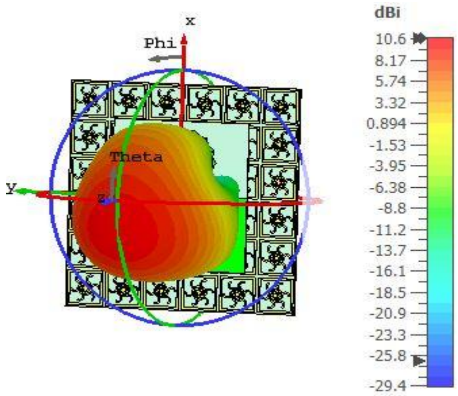

Fig. 6 – Shows the far-field radiation pattern at 5 GHz, featuring a broadside main lobe with a peak realized gain of 10.4-10.6 dBi, nearly symmetrical *E*- and *H*-plane patterns, an HPBW of 58°-60°, and a suppressed back-lobe below – 15 dB, resulting in an FBR of 16-18 dB

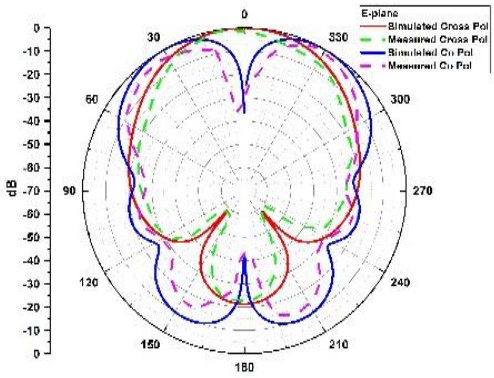

a

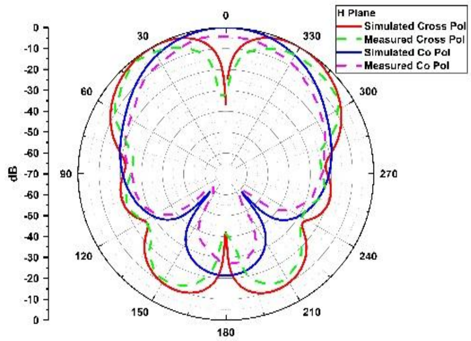

b

Fig. 6(i) – (a) *E*-plane & (b) *H*-plane radiation patterns of the suggested antenna at 5 GHz

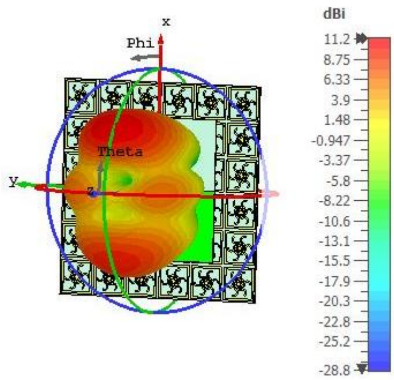

a

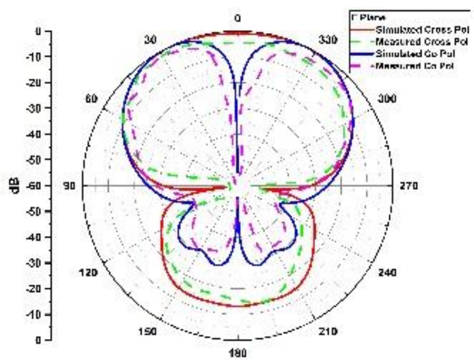

b

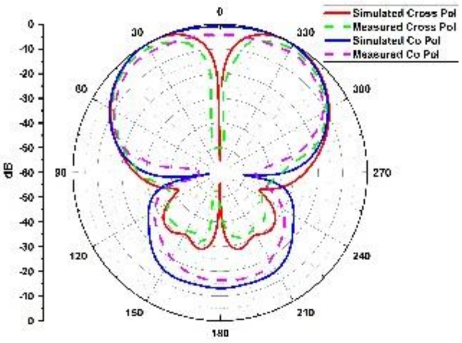

c

Fig. 6(ii) – (a) 3D gain, (b) *E*-plane & (c) *H*-plane radiation patterns of the suggested antenna at 10 GHz

At 10 GHz (Fig. 6(ii)), the antenna exhibits a more directive broadside radiation with a peak gain of 11.2 dBi, a reduced HPBW of 44°-48°, and back-lobe suppression below – 18 dB, yielding an FBR of 18-20 dB. The beam narrowing at higher frequency is attributed to the increased electrical aperture, confirming suitability for high-gain point-to-point microwave communication.

7. THE ANTENNA–FSS CONFIGURATION SURFACE CURRENT DISTRIBUTIONS

Fig. 7 (a) and (b) depict the simulated surface current distribution of the suggested antenna integrated with the FSS.

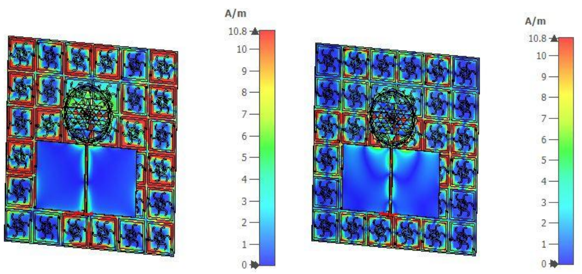

a b

Fig. 7 – SCD (Surface current distribution) showing electromagnetic coupling between the antenna and the FSS superstrate

Fig. 7 shows a strong surface-current concentration along the feed line, the fractal radiator, and the inner edges of the FSS unit cells, confirming efficient antenna-FSS coupling. The peak current density reaches 10-10.8 A/m in Fig. 7(a) & 9.5-10.5 A/m in Fig. 7(b), while moderate currents of 3-7 A/m appear on adjacent FSS elements. In contrast, the outer regions show low current levels (< 2-3 A/m), indicating suppressed surface waves and reduced back radiation. This controlled current distribution validates the gain-enhancement mechanism, resulting in improved front-to-back ratio.

8. CONCLUSION

A compact Srichakra-shaped fractal wideband monopole antenna integrated with a 6 × 6 FSS reflector and a 20 mm air gap is presented for gain enhancement. Without the FSS, the antenna achieves wide impedance bandwidth with a realized gain of 5.3-8.6 dBi over 2-20 GHz, while FSS integration improves the peak gain to 11.6-11.8 dBi at 10 GHz, providing a consistent enhancement of 1.6-3.6 dB across the band. The front-to-back ratio increases to 18-20 dB, and surface current analysis confirms constructive field reinforcement with peak currents exceeding 10 A/m. The wideband impedance matching is preserved with only minor resonance shifts, demonstrating that the proposed antenna-FSS configuration is a compact, low-profile, and high-gain solution for wideband point-to-point microwave and data-link communication applications.

Comparison Table

Ref	Material	Bandwidth (GHz)	Peak gain(dBi)
[3]	FR-4	3.0 to 11.0	8.3
[6]	FR-4	5.0 to 14.0	10.5
[8]	RO435OB	2.0 to 16.0	9.2
[9]	RO4350B	9.0 to 12.5	9.8
[14]	RO4003C	8.0 to 15.0	8.5
This work	RO4350B	2.0 to 20.0	11.6

The comparison shows that most reported FSS-based antennas operate over 3-15 GHz with peak gains below 10.5 dBi. In contrast, the proposed RO4350B-based design achieves a much wider 2-20 GHz bandwidth with a higher peak gain of 11.6 dBi, demonstrating its superior wideband and gain performance over existing works.

ACKNOWLEDGEMENT

The authors express their sincere gratitude to DST for giving support through File No. SR / PURSE / 2023 /196 & SR / FST / ET-II / 2019 /450.

REFERENCES

1. M.F. Ahmed, M.H. Kabir, *Cureus J.* **2** No 1, (2025) https://doi.org/10.7759/s44388-025-03326-4.
2. S. Attioui, A. Khabba, S. Ibnyaich, A. Zeroual, Z. Zakaria, A.J. Al-Gburi, *Progr. Electromagn. Res. C* **155**, 203 (2025) https://doi.org/10.2528/PIERC25022001.
3. M.D. Lanka, S. Chalasani, *Eng. Proc.* **59** No 1, 143 (2024) https://doi.org/10.3390/engproc2023059143.
4. O. Benkhadda, M. Saih, S. Ahmad, A.J. A. Al-Gburi, Z. Zakaria, K. Chaji, A. Reha, *Fractal and Fractional* **7** No 2, 115 (2023) https://doi.org/10.3390/fractalfract7020115.
5. R. Aradhyula, T.R. Krishna, B.T.P. Madhav, *Int. J. Eng. Adv. Technol.* **8** No 6, 1986 (2019) https://doi.org/10.1007/978-981-16-0695-3_5.
6. I.U. Din, S. Ullah, S.I. Naqvi, R. Ullah, S. Ullah, E.M. Ali, M. Alibakhshikenari, *Int. J. Antennas Propag.* **2022** No 1, 2002552 (2022) https://doi.org/10.1155/2022/2002552.
7. A.J.A. Al-Gburi, I.M. Ibrahim, Z. Zakaria, M.K. Abdulhameed, T. Saeidi, *Mathematics* **9** No 24, 3301 (2021) https://doi.org/10.3390/math9243301.
8. M. Hussain, M.A. Sufian, M.S. Alzaidi, S.I. Naqvi, N. Hussain, D.H. Elkamchouchi, S.Y.A. Fatah, *Microm-*

achines **14** No 3, 591 (2023).
9. C.R. Sereddy, U.D. Yalavarthi, T.P.M. Boddapati, *Joint J. Novel Carbon Resource Sci. Green Asia Strategy* **12** No 02, 1079 (2025) https://doi.org/10.5109/7363496.
10. R.K. Dash, P.B. Saha, D. Ghoshal, G. Palai, *Wireless Networks* **29** No 2, 589 (2023) https://doi.org/10.1109/ACCESS.2023.3243292.
11. A.K. Verma, R. Singhal, *Wireless Pers. Commun.* **135** No 1, 517 (2024) https://doi.org/10.1007/s11277-024-11080-9.
12. G. Bharti, J.S. Sivia, *Wireless Pers. Commun.* **137** No 4, 2535 (2024) https://doi.org/10.1007/s11277-024-11521-5.
13. S.R. Ghali, B.T.P. Madhav, M. Alathbah, P. Pardhasaradhi, N. Prasad, *J. Electron. Mater.* **53** No 3, 1660 (2024) https://doi.org/10.1007/s11664-023-10823-x.
14. M. Singh, H. Singh, *Aerospace Syst.* **5** No 4, 663 (2022) https://doi.org/10.1007/s42401-022-00163-9.

Проєктування широкосмугової антени у формі Шрічакри з посиленим підсиленням на основі FSS для мікрохвильових ліній передачі даних "точка-точка"

Ghali Srinivasa Rao[1], B.T.P. Madhav[1], Y. Usha Devi[1], Geetha Reddy Yenna[2], K Jyostna[3], Lokesh Raju V[4]

[1] *ALRC Research Centre, Department of ECE, Koneru Lakshmaiah Education Foundation, Guntur, 522302 Andhra Pradesh, India*
[2] *Malla Reddy Engineering College for Women (MRECW), Hyderabad, India*
[3] *Department of ECE, VNR VJIET, Hyderabad, India*
[4] *Department of ECE, Adithya Institute of Technology and Management (AITM), Tekkali, AP, India*

Для широкосмугового мікрохвильового зв'язку "точка-точка" реалізовано компактну планарну антену, натхненну Шрічакрою, у поєднанні з частотно-селективною поверхнею (ЧПС). Запропонована антена використовує діелектрик Rogers RO4350B, що займає компактний об'єм 46 × 51,5 × 0,3 мм³. Для посилення прямого випромінювання як пасивний суперстрат використовується спіральний резонатор ЧПС, натхненний фракталами. Елементарна комірка ЧПС утворена періодичністю 12 × 12 мм² та реалізована на підкладці RO4350B товщиною 0,4 мм. Сформовано решітку ЧПС 6 × 6, що призводить до загальних розмірів 78 × 78 мм². Така схема функціонує як компактна широкосмугова частково відбиваюча поверхня. ЧПС перенаправляє зворотне випромінювання у прямий півпростор завдяки конструктивній взаємодії поля. В результаті досягається стабільне посилення в широкому діапазоні робочих частот. Реалізований коефіцієнт підсилення збільшується з 6,9 дБі без FSS до пікового значення 11,2 дБі з FSS. Це відповідає максимальному покращенню коефіцієнта підсилення приблизно на 3 дБ. Антена зберігає стабільне узгодження імпедансу та поведінку випромінювання після інтеграції FSS. Постійно високий коефіцієнт підсилення спостерігається в усьому діапазоні 5-20 ГГц. Використання матеріалів з низькими втратами та пасивний механізм підсилення забезпечує високу ефективність випромінювання. Загалом, розроблена антена пропонує компактну, широкосмугову конструкцію з високим коефіцієнтом підсилення, придатну для систем мікрохвильового зв'язку "точка-точка".

Ключові слова: ЧСП (частотно-селективна поверхня), Підсилення, Мікрохвильовий зв'язок каналу передачі даних, Зв'язок "точка-точка", Широкосмугова антена.